Lensing Constraints on Galaxy Cluster Mass and Structure

Graham P. Smith

gps@star.sr.bham.ac.uk

University of Birmingham

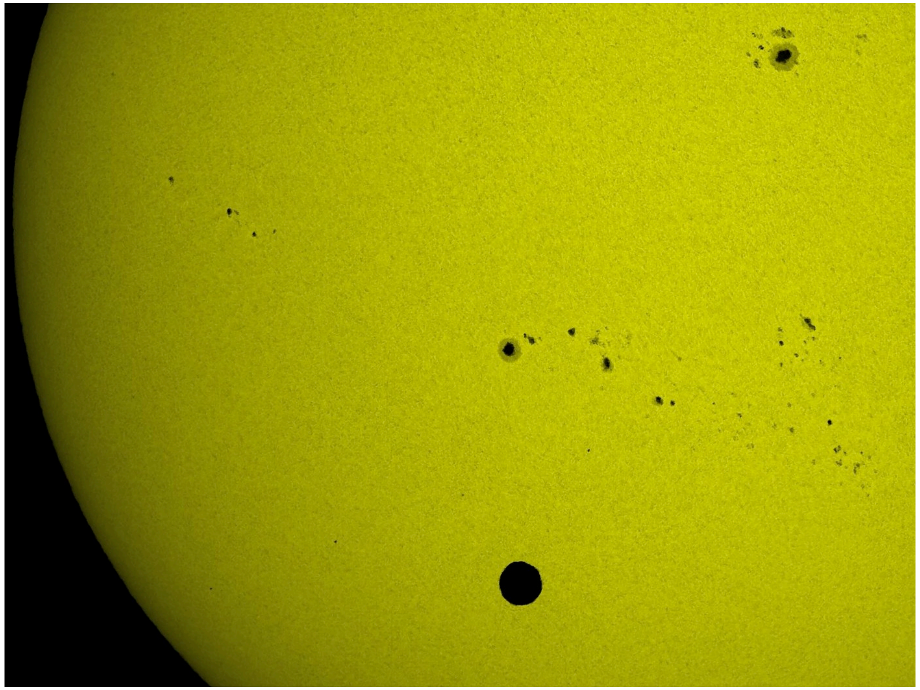

1. Primer on the physics of galaxy clusters

2. Galaxy clusters as cosmological probes

3. Galaxy clusters as gravitational lenses

Part 1:

Primer on the
Physics of Galaxy Clusters

Overview

- Composition of galaxy clusters
- Origin and properties of intracluster medium
- Spherical collapse model
- Dark matter halo mass function
- Self-similar model
- Mass-observable scaling relations
- X-ray mass measurements
- Self-similar density profiles

Composition of galaxy clusters

the largest collapsed structures in the Universe

Large clusters should provide a "fair sample" of the matter in the universe which is able to cluster – i.e. the baryonic and dark matter.

Typically: 85% of cluster mass is dark matter
~80% of the *baryonic* matter is in hot gas

Composition of the Universe:

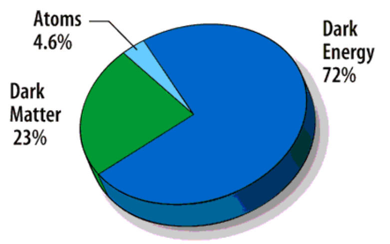

Composition of clusters:

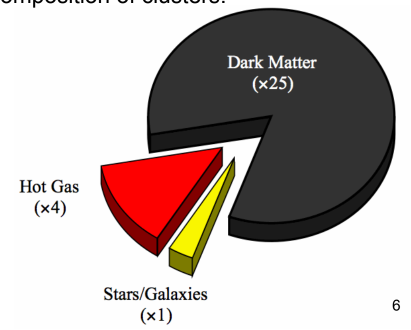

Composition of galaxy clusters

the largest collapsed structures in the Universe

- Total masses = $10^{14} – 10^{15}\ M_\odot$
  - How do you define (and measure) the mass of a cluster?
- Dark matter:
  - 85% of matter in clusters is "missing mass" / dark matter
- Galaxy content:
  - hundreds of luminous ($\geq 10^{10}\ L_\odot$) galaxies
  - only ~5 – 10% of galaxies are found in clusters
  - 30 – 50% of galaxies in a galaxy groups (M_{virial}~$2\text{x}10^{12} – 10^{14}\ M_\odot$)
- X-ray emitting atmosphere (intracluster medium):
  - 80% of cluster baryons are in a hot ionized plasma
  - ~$2\text{x}10^{7} – 10^{8}$ K, i.e. 2 – 10 keV
- Intracluster light:
  - stars that lie in between galaxies
- Distinction between groups and clusters is arbitrary
  - typical cut-off: M ~ $10^{14}\ M_\odot$ or an T_X ~ 2keV.

Central cDs and intracluster light

Many clusters, and some galaxy groups, have a dominant ellipical (known as a cD – for "central-Dominant") near the centre, which is surrounded by an extended diffuse stellar halo. M87, in the Virgo cluster, is an example.

Central cDs and intracluster light

The diffuse light within such clusters used to be thought of as a stellar halo surrounding the central cD, but more recently it has been realised that this light may be highly structured, and pervade the whole cluster, as seen in this image of Virgo.

This has led to it being referred to as intracluster light (ICL).

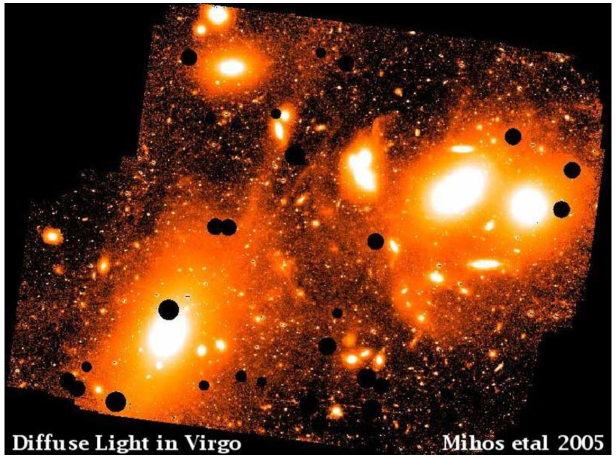

Global properties

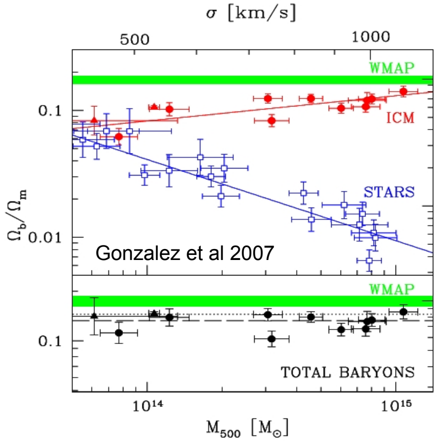

What looks odd about this plot?

The balance between stars and gas is observed to vary substantially from groups to clusters.

The hot gas fraction rises with system mass, whilst the stellar mass fraction falls. In poor groups, the two are approximately equal.

The *total* baryon fraction seems to be rather less than the cosmic mean value of 17% (from WMAP).

Whether f_{baryon} drops in groups is controversial.

What is the origin of the ICM?

– a simple model of cluster formation –

- Galaxies form by baryon cooling within dark halos
- These then cluster into groups which grow into clusters
- Galaxy dark halos merge
- Infalling gas is compressed and shocked at R_{virial}

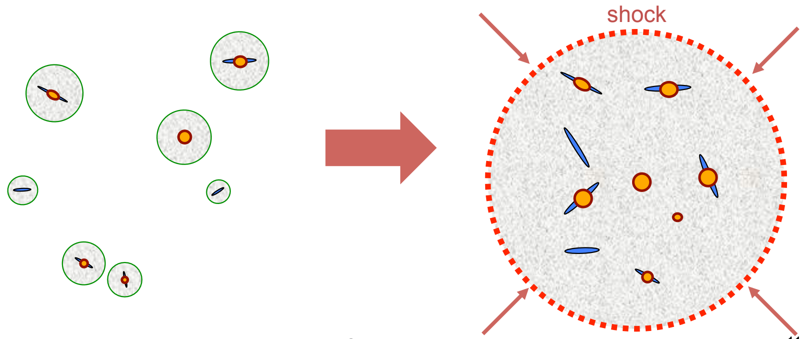

What looks odd about this cartoon?

Virial temperature of the ICM

$$T \approx \left(\frac{\sigma}{1000\,\mathrm{km\,s^{-1}}}\right)^2 \times 6.2\ \mathrm{keV}$$

- σ = velocity dispersion of the cluster (typical speed at which galaxies move)
- Try to derive this expression
- Hint:
  - assume that the specific energy of the galaxies and the ICM are roughly equal
  - why is that a reasonable thing to do?

Emission mechanisms

ICM is an optically thin plasma that radiates through a combination of bremsstrahlung and atomic line emission.

The bremsstrahlung emissivity has the form:

$$\epsilon(E) = A\,(\sum_i Z_i^2 n_e n_i)\,T^{1/2} g(T,E) e^{-E/kT},$$

where for gas of temperature T, the Gaunt factor is a slowly varying function of energy: $g(T,E) \propto E^{-0.4}$

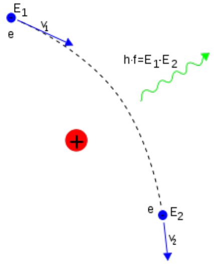

Line emission starts to dominate in cooler systems: T<~3keV

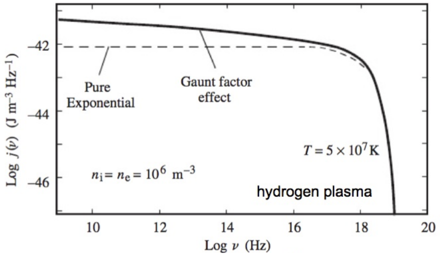

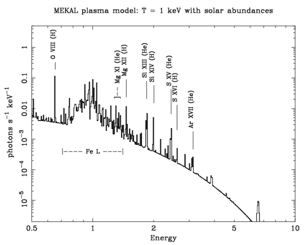

Defining galaxy cluster mass

- What do we mean by "mass of a cluster"?
- Ideally we want to add up all the mass, meaning:
  - **<u>all kinds</u>** of matter (luminous and dark) …
  - that is **<u>inside</u>** the cluster
- What do we mean by "inside the cluster"?
- Where is the edge of a cluster?

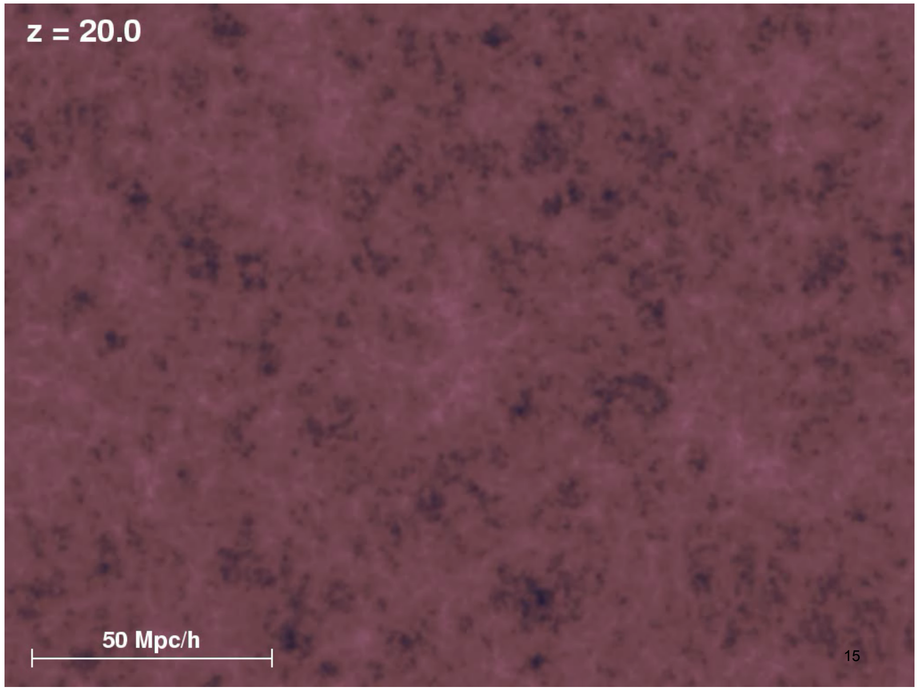

Spherical Collapse Model

Consider a uniform spherical density perturbation – a spherical top hat:

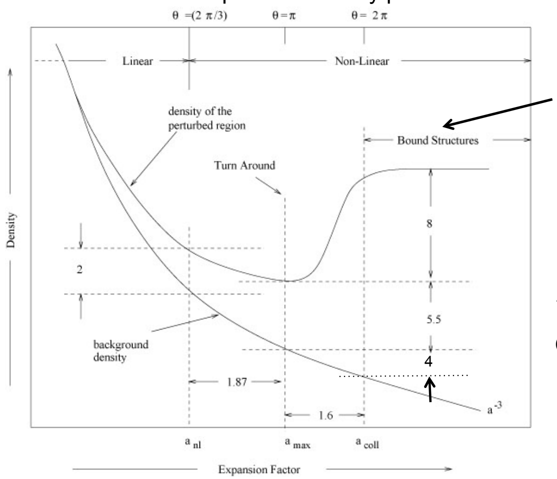

Virialized structures – meaning they obey the virial theorem

$$R_{ta} = 2R_{virial} \Rightarrow \frac{\rho_{virial}}{\rho_{ta}} = 8$$

$$\Delta_{virial} = \frac{\rho_{virial}}{\rho_{crit}} = 8 \times 5.5 \times 4 = 178$$

(for EdS Universe)

Virial radius is a common working definition of the "edge" of a cluster

Padmanabhan arXiv:hep-th/0212290

Virial radius

- Definition:
  - Radius within which the cluster obeys the virial theorem
  - Radius within which the mean cluster density is: virial over-density x critical density

$$\left\langle \rho(< r_{virial}) \right\rangle = \Delta_{virial} \rho_{crit}$$

Virial over-density in ΛCDM

- For a flat universe with cosmological constant: (Bryan & Norman, 1998)

$$\Delta_{\mathrm{virial}} = 18\pi^2 + 82\left[\Omega_{\mathrm{m}}(z) - 1\right] - 39\left[\Omega_{\mathrm{m}}(z) - 1\right]^2$$

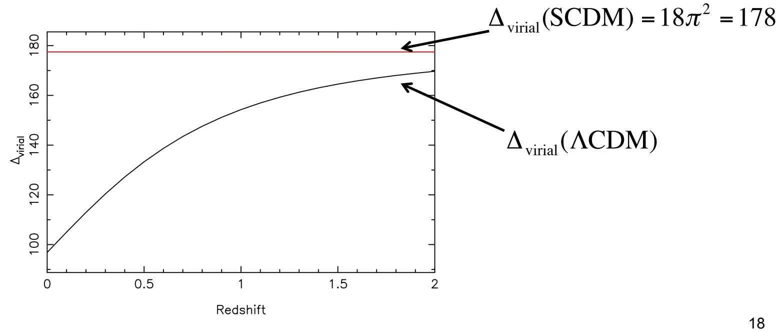

Virial mass

We can therefore write this expression for the virial mass of a cluster:

$$M_{virial} = \frac{4\pi r_{virial}^3}{3} \Delta_{virial} \rho_{crit}$$

More generally, we can define an “over-density” mass:

$$M_{\Delta} = \frac{4\pi r_{\Delta}^3}{3} \Delta \rho_{crit}$$

Common over-densities include: 200, 500, 2500

Which of these radii is the smallest?: r_{virial} r_{200} r_{500} r_{2500}

From this we obtain a convenient scaling between mass and radius:

$$M_{\Delta} \propto r_{\Delta}^3$$

Press & Schechter 1976

Mass function

$$\frac{dn}{dM}(M,t) = \frac{2\bar{\rho}\delta_c}{M^2}\frac{1}{\sqrt{2\pi}\sigma_M}\left|\frac{dln\sigma_M}{dlnM}\right| \exp\left(\frac{-\delta_c^2}{2\sigma_M^2}\right)$$

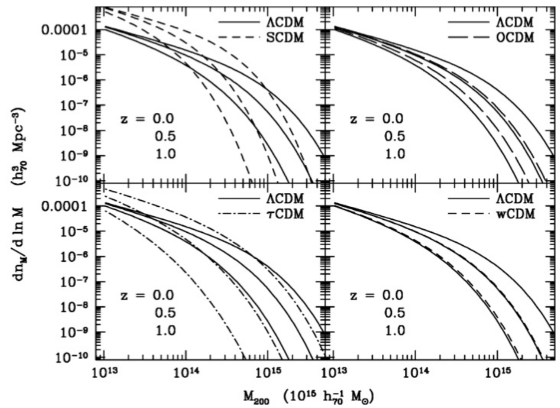

FIG. 5. Mass-function evolution in five different cosmologies. The fiducial model in all cases is the ΛCDM model with $\Omega_M=0.3$, $\Omega_\Lambda=0.7$, $w=-1$, and $\sigma_8=0.9$. Upper left: panel compares cluster evolution in the ΛCDM case with a standard cold-dark-matter model (SCDM) having $\Omega_M=1.0$, $\Omega_\Lambda=0.0$, and $\sigma_8=0.5$. Evolution in the SCDM case is much more dramatic, and the steeper slope of the mass function strongly disagrees with observations of local clusters (Reiprich and Böhringer, 2002). Lower left: retaining $\Omega_M=1.0$ and $\Omega_\Lambda=0.0$ while adjusting the power spectrum so that $\Gamma=0.21$ gives a τCDM model in which the slope of the low-redshift mass function is more acceptable, but the evolution is still very strong. Upper right: dispensing with dark energy while keeping the matter density low gives an OCDM model ($\Omega_M=0.3$, $\Omega_\Lambda=0$, $\sigma_8=0.9$) with less evolution than the ΛCDM case because structure formation starts to ramp down earlier in time (see Fig. 2). Lower right: dark energy in a wCDM model identical to the ΛCDM model except with $w=-0.8$ also slows cluster evolution relative to the ΛCDM case.

Galaxy clusters occupy the exponential tail of the halo mass function

Voit 2005

Self similar model

- A simple model to relate galaxy cluster mass to observable quantities
- Assumes that cluster properties are determined by solely gravitational physics
  – Gravitational collapse of DM halos
  – Infall of galaxies and gas
  – Shock heating of intracluster gas

Self similar model

Apply virial theorem to galaxies orbiting in the cluster potential:

$$M_{virial} \propto \sigma_{los}^2 r_{virial}$$

In virial equilibrium the specific energy of ICM equals specific energy of galaxies, from which we can show:

$$T_X \propto \sigma_{los}^2 \Rightarrow M_{virial} \propto T_X r_{virial}$$

Remember that mass is proportional to volume (r^3), to obtain:

$M_{virial} \propto T_X^{3/2}$ More generally: $M_\Delta \propto T_X^{3/2}$

Think about: how would this relation change if mass is measured within a radius of fixed size?

Self similar model

X-ray luminosity of a cluster depends on density, size, and T_X:

$$L_X \propto n_e n_i V \Lambda(T_X) \propto r_{virial}^3 T_X^{1/2}$$

The mass-temperature relation (previous slide) implies a temperature-size relation:

$$r_{virial}^3 \propto T_X^{3/2} \Rightarrow L_X \propto T_X^2$$

Combining the L-T and M-T relation, we obtain the M-L relation:

$M_{virial} \propto L_X^{3/4}$ More generally: $M_\Delta \propto L_X^{3/4}$

But clusters are not self-similar
(on all scales)

Gas cools more quickly at higher density, and gas is heated by AGN in cluster cores

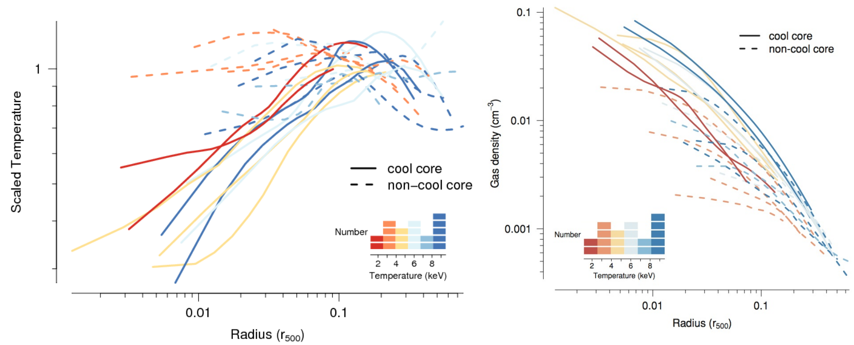

$$t_{cool} \propto \frac{E_{thermal}}{\varepsilon} \propto \frac{\rho_{gas} T}{\rho_{gas}^2 \Lambda} \propto \frac{T^{0.5}}{\rho_{gas}}$$

"Cool cores"
"AGN feedback"

Sanderson, O'Sullivan, Ponman, 2009

Example scaling relation slopes

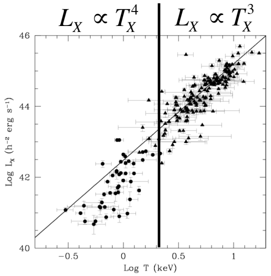

Mulchaey, 2000, ARA&A

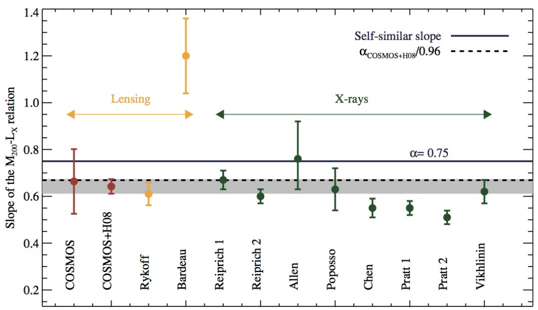

Leauthaud et al., 2010

Self-similar evolution

Remember: $$M(<r_\Delta) = \frac{4\pi r_\Delta^3}{3}\rho_{crit}\Delta$$

Critical density depends on redshift: $$\rho_{crit}(z) = \frac{3H(z)^2}{8\pi G}$$

$$H(z) = H_0\left[\Omega_M(1+z)^3 + \Omega_\Lambda\right]^{1/2} = H_0 E(z)$$

Two options regarding over-density:

(1) Fixed value, e.g. 200, 500, 2500

(2) Virial over-density $$\Delta_{\mathrm{virial}}(z) = 18\pi^2 + 82\left[\Omega_m(z) - 1\right] - 39\left[\Omega_m(z) - 1\right]^2$$

$$\Omega_m(z) = \frac{\Omega_M(1+z)^3}{E(z)^2}$$

Self-similar evolution

Putting it all together from previous slides:

$$M_\Delta \propto T_X^{3/2} E(z)^{-1} \Delta_z^{-1/2}$$

$$L_X \propto T_X^2 E(z) \Delta_z^{1/2}$$

$$M_\Delta \propto L_X^{3/4} E(z)^{-7/4} \Delta_z^{-7/8}$$

$$\Delta_z = \Delta(z=0)\frac{\Delta_{virial}(z)}{\Delta_{virial}(z=0)}$$

M-T evolution is consistent with self-similar, but beware selection effects and mass measurement systematics …

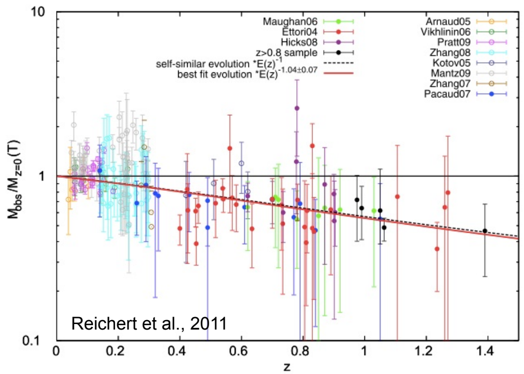

Fig. 3. Redshift evolution of the M–T relation. Black-dashed line: self-similar prediction ($\propto E(z)^{-1}$). Continuous red line: best-fit evolution ($\propto E(z)^{-1.04\pm0.07}$).

X-ray mass measurements

Basic idea:

assume the ICM is in **hydrostatic equilibrium** with a **spherical** gravitational potential, and infer mass from the pressure gradient.

$$\frac{dP}{dr} = -\frac{GM(<r)\rho}{r^2} \Rightarrow M(<r) = -\frac{rkT(r)}{G\mu m_p}\left[\frac{d\ln\rho}{d\ln r} + \frac{d\ln T}{d\ln r}\right]$$

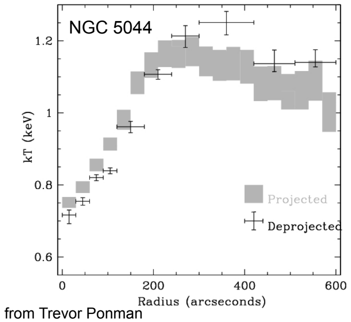

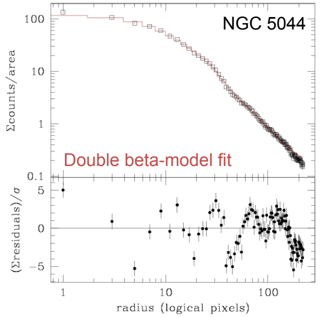

Figures from Trevor Ponman

Self-similar density profile?

Navarro, Frenk, White, 1997

The density profile of "equilibrium" dark matter halosin DM-only numerical simulations is independent of mass and cosmology.

Density profile: $\dfrac{\rho(r)}{\rho_{crit}} = \dfrac{\delta_c}{(r/r_s)(1+r/r_s)^2}$

Characteristic density: $\delta_c = \dfrac{\Delta}{3}\dfrac{c_\Delta^3}{\ln(1+c_\Delta) - c_\Delta/(1+c_\Delta)}$

Concentration: $c_\Delta = \dfrac{r_\Delta}{r_s}$

$\rho \propto r^{-2}$ at $r = r_s$ (the scale radius)

$\rho \to r^{-1}$ at $r << r_s$

$\rho \to r^{-3}$ at $r >> r_s$

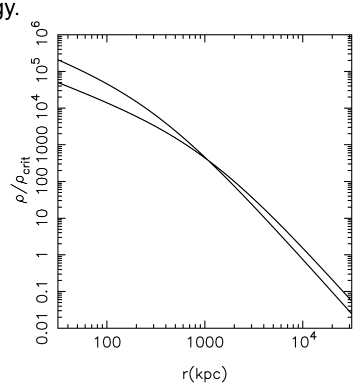

Which of these density profiles has the higher concentration parameter?

Self-similar density profile?

- Density profile is cuspy in the center
  - slope is hotly debated by simulators
- Density profile is curved
  - dark matter distribution is not isothermal
- Density profiles are self-similar
  - a consequence of collisionless dark matter (and the absence of baryons from the simulation?)
- Concentration is anti-correlated with mass
  - Duffy et al., 2008, Neto et al., 2007, Dolag et al., 2004, Bullock et al., 2001, …
  - a consequence of hierarchical assembly in an expanding universe

Why?

$$c_\Delta \propto M_\Delta^{-0.1}$$

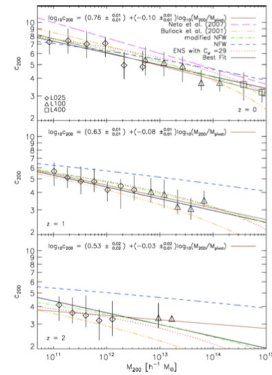

Figure 2. Concentration–mass relations for $z = 0$ (top panel), 1 (middle panel) and 2 (bottom panel) using NFW density profiles. Data points correspond to median values and errorbars to quartiles. Only bins containing at least five haloes are shown. The black, solid lines show the best-fitting power-law relation. The errors on the best-fitting parameters, given in the legend, are determined by bootstrap resampling the haloes and correspond to 68.2 per cent confidence limits. The pink dashed line in the top panel shows the best-fitting power-law relation to all haloes from N07. The other curves represent the prescriptions discussed in Section 3.1. The brown solid lines correspond to the special case where we set $C = 0$ in equation (4), and fitted a power law to the data at each individual redshift.

Summary

- Galaxy clusters contain:
  - a fair sample of the content of universe
  - DM, galaxies, intracluster stars, hot gas
- Galaxy clusters inhabit the exponential tail of the DM halo mass function
- Galaxy clusters are therefore powerful cosmological tools
- Cluster cosmology would be easy (and boring!) if clusters are self-similar
- Cluster masses can be inferred from X-ray (and optical) observations by assuming relationship between baryons and DM
- Departures from self-similarity → lots of interesting physics

Part 2

Galaxy Clusters as Cosmological Probes

– examples and mass measurement issues –

Overview

- Examples of cluster-based cosmological constraints
  - Dark matter
  - Low density universe
  - Nature of dark matter
  - Dark energy
- Mass measurement issues
  - Critique of cluster mass measurement in state of the art cluster-based DE constraints

THE MASS OF THE VIRGO CLUSTER*

SINCLAIR SMITH

ABSTRACT

The lists of radial velocities now include results for thirty-two members of the Virgo Cluster, thus giving for the first time sufficient data to determine some of the physical characteristics of a cluster of nebulae.

A comparison of the velocities of fainter members of the cluster with those of brighter members shows that the line-of-sight velocity of a nebula has no dependence on its magnitude; hence, equipartition apparently does not hold in the cluster. The distribution of the velocities in right ascension and declination shows that the cluster is not in rotation and that there is no central concentration of high velocities. This result is taken to mean that the cluster is neither condensing nor breaking up, but is a fairly stable assemblage, more or less held together by its gravitational field.

From the observed distribution function for radial velocity is derived the distribution function for space velocity. For an assumed distance of 2×10^6 parsecs this function leads to 2×10^{47} g or 10^{14} $\odot$ as a value of the mass of the cluster. On the basis of 500 nebulae in the cluster, the mass per nebula is 2×10^{11} $\odot$.

Although far larger than Hubble's value of 10^9 $\odot$ for the mass of an average nebula, other evidence lends support to the high value obtained from the Virgo Cluster. It is possible that both figures are correct and that the difference represents a great mass of internebular material within the cluster.

[4] *Mt. W. Comm.*, No. 105; *Proc. Nat. Acad.*, **15**, 168, 1929.

[5] I am indebted to Dr. Hubble for suggesting this point.

[6] F. Zwicky has pointed out (*Helv. Phys. Acta*, **6**, No. 2, p. 110, 1933) that the velocity range in the Coma Cluster indicates non-luminous matter which is some four hundred times the amount of the observed luminous material.

[7] Stebbins, *Mt. W. Comm.*, No. 113; *Nat. Acad. Proc.*, **20**, 93, 1934.

Smith, 1936, ApJ, 83, 23

ON THE MASSES OF NEBULAE AND OF CLUSTERS OF NEBULAE

F. ZWICKY

ABSTRACT

Present estimates of the masses of nebulae are based on observations of the *luminosities* and *internal rotations* of nebulae. It is shown that both these methods are unreliable; that from the observed luminosities of extragalactic systems only lower limits for the values of their masses can be obtained (sec. i), and that from internal rotations alone no determination of the masses of nebulae is possible (sec. ii). The observed internal motions of nebulae can be understood on the basis of a simple mechanical model, some properties of which are discussed. The essential feature is a central core whose internal *viscosity* due to the gravitational interactions of its component masses is so high as to cause it to rotate like a solid body.

In sections iii, iv, and v three new methods for the determination of nebular masses are discussed, each of which makes use of a different fundamental principle of physics.

Method iii is based on the *virial theorem* of classical mechanics. The application of this theorem to the Coma cluster leads to a minimum value $\overline{M}=4.5\times10^{10}M_\odot$ for the average mass of its member nebulae.

Method iv calls for the observation among nebulae of certain *gravitational lens* effects.

Section v gives a generalization of the principles of ordinary *statistical mechanics* to the whole system of nebulae, which suggests a new and powerful method which ultimately should enable us to determine the masses of all types of nebulae. This method is very flexible and is capable of many modes of application. It is proposed, in particular, to investigate the distribution of nebulae in individual great clusters.

As a first step toward the realization of the proposed program, the Coma cluster of nebulae was photographed with the new 18-inch Schmidt telescope on Mount Palomar. Counts of nebulae brighter than about $m=16.7$ given in section vi lead to the gratifying result that the distribution of nebulae in the Coma cluster is very similar to the distribution of luminosity in globular nebulae, which, according to Hubble's investigations, coincides closely with the theoretically determined distribution of matter in isothermal gravitational gas spheres. The high central condensation of the Coma cluster, the very gradual decrease of the number of nebulae per unit volume at great distances from its center, and the hitherto unexpected enormous extension of this cluster become here apparent for the first time. These results also suggest that the current classification of nebulae into relatively few *cluster nebulae* and a majority of *field nebulae* may be fundamentally inadequate. From the preliminary counts reported here it would rather follow that practically *all* nebulae must be thought of as being grouped in clusters—a result which is in accord with the theoretical considerations of section v.

In conclusion, a comparison of the relative merits of the three new methods for the determination of nebular masses is made. It is also pointed out that an extensive investigation of great clusters of nebulae will furnish us with decisive information regarding the question whether physical conditions in the known parts of the universe are merely fluctuating around a stationary state or whether they are continually and systematically changing.

Zwicky 1937

Citations history for 1933AcHPh...6..110Z from the ADS Databases

The Citation database in the ADS is **NOT** complete. Please keep this in mind when using the ADS Citation lists.

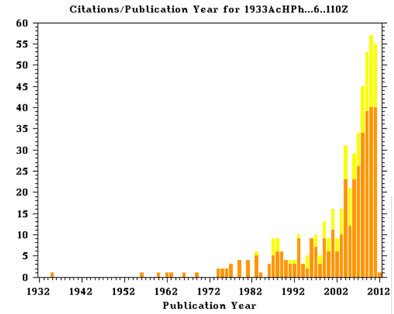

Citations history for 1936ApJ....83...23S from the ADS Databases

The Citation database in the ADS is **NOT** complete. Please keep this in mind when using the ADS Citation lists.

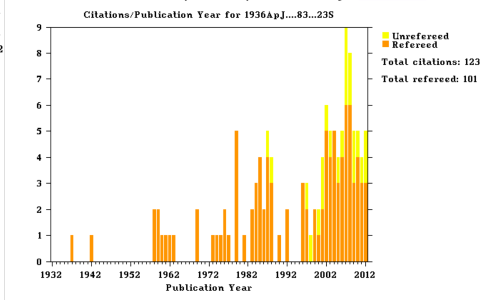

The baryon content of galaxy clusters: a challenge to cosmological orthodoxy

Simon D. M. White*, Julio F. Navarro†, August E. Evrard‡ & Carlos S. Frenk†

* Institute of Astronomy, Madingley Road, Cambridge CB3 0HA, UK
† Department of Physics, University of Durham, Durham DH1 3LE, UK
‡ Department of Physics, University of Michigan, Ann Arbor, Michigan 48109, USA

Baryonic matter constitutes a larger fraction of the total mass of rich galaxy clusters than is predicted by a combination of cosmic nucleosynthesis considerations (light-element formation during the Big Bang) and standard inflationary cosmology. This cannot be accounted for by gravitational and dissipative effects during cluster formation. Either the density of the Universe is less than that required for closure, or there is an error in the standard interpretation of element abundances.

Flat, matter dominated flat universe combined with primordial nucleosynthesis:

$$\Omega_{baryon} = \frac{\rho_{baryon}}{\rho_{crit}} = 0.0125\ h^{-2}$$

Inventory of galaxies, gas, plus X-ray/dynamical estimates of total mass, and assumption that cluster content is representative of the universe:

$$f_{baryon} = \frac{M_{galaxies} + M_{gas}}{M_{total}} \approx 0.06\ h^{-1.5}$$

White et al., 1993

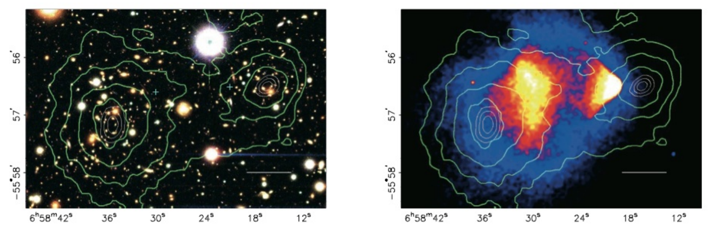

Fig. 1.—*Left panel*: Color image from the Magellan images of the merging cluster 1E 0657−558, with the white bar indicating 200 kpc at the distance of the cluster. *Right panel*: 500 ks *Chandra* image of the cluster. Shown in green contours in both panels are the weak-lensing κ reconstructions, with the outer contour levels at $\kappa = 0.16$ and increasing in steps of 0.07. The white contours show the errors on the positions of the κ peaks and correspond to 68.3%, 95.5%, and 99.7% confidence levels. The blue plus signs show the locations of the centers used to measure the masses of the plasma clouds in Table 2.

Clowe et al., 2006 – “Direct evidence for the existence of Dark Matter”

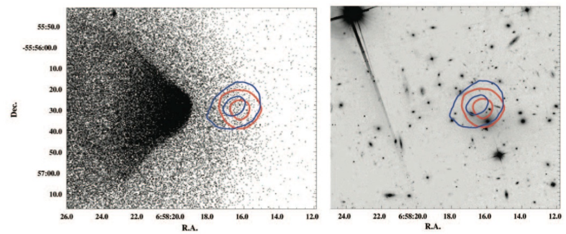

$$\frac{\sigma}{m} \leq 0.7\ cm^2/g$$

Fig. 2.—Close-up of the subcluster bullet region, with the DM (*blue*) and galaxy (*red*) centroid error contours overlain. The contours show the 68.3% and 99.7% error regions. The left panel shows the X-ray *Chandra* image, while the right shows the optical *HST* image.

Randall et al., 2008 – constraints on the cross-section of DM to self-interaction

Thanks to Nigel Watson, Birmingham & CERN

The bullet in context

Convert cross-section to self-interaction to particle physics units:

$$1\ cm^2/g = 1\ /\ (0.931/1.66\times10^{-24})\ cm^2/GeV = 1.8\times10^{-24}\ \mathrm{cm}^2/GeV = 1.8\times10^{12}\ \mathrm{pb}/GeV$$

For illustrative purposes, assume DM candidate has mass comparable with electroweak scale (100GeV): $\sigma_{SI} \leq 1.8\times10^{9}\,pb$

This is huge!! Comparable to proton-proton inelastic cross-section at LHC!!

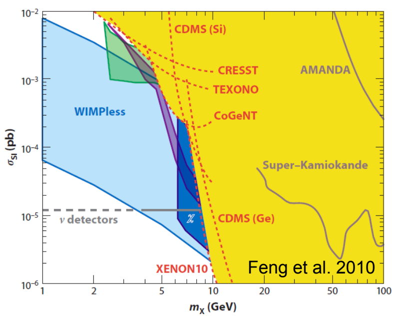

Direct detection experiments target DM-nucleon cross-sections of ~10^{-6} – 10^{-2}pb

The only direct evidence for the existence of DM comes from astrophysical observations

Impossible to test DM-DM self-interaction in any other way than via astrophysical observations

Dark Energy

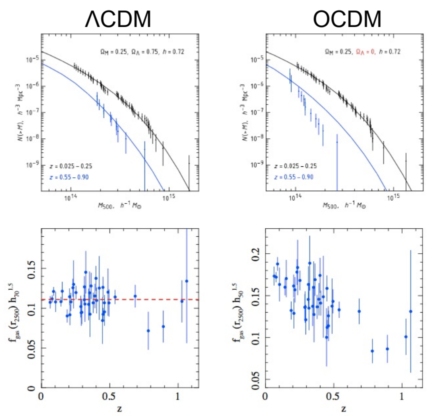

<u>Growth of structure</u>

(see Cristiano’s 3rd lecture)

Relies on scaling relations and unrealistic simulations

<u>Expansion history of universe</u>

$$f_{gas} \propto D_L D_A^{0.5}$$

f_{gas} **assumed** not to evolve
But it is a function of mass!

Figure 9: Examples of cluster data used in recent cosmological work. *Top*: Measured mass functions of clusters at low and high redshifts are compared with predictions of a flat, ΛCDM model and an open model without dark energy (from Vikhlinin et al. 2009b). *Bottom*: $f_{gas}(z)$ measurements for relaxed clusters are compared for a $\Omega_m = 0.3$, $\Omega_\Lambda = 0.7$, $h = 0.7$ model (*left*, consistent with the expectation of no evolution) and a $\Omega_m = 1.0$, $\Omega_\Lambda = 0.0$, $h = 0.5$ model (*right*; from Allen et al. 2008). For purposes of illustration, cosmology-dependent derived quantities are shown (mass and f_{gas}); in practice, model predictions are compared with cosmology-independent measurements.

Allen et al., 2011, ARA&A

Reliability of cluster masses

- In principle:
  - Count clusters as function of mass and redshift
- In reality:
  - As a function of a mass-like observable and redshift
  - Use a mass-observable scaling relation to get mass

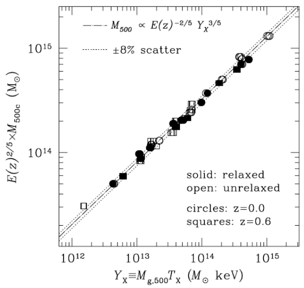

Kravtsov et al., 2006

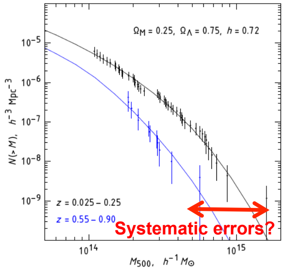

Vikhlinin et al., 2009

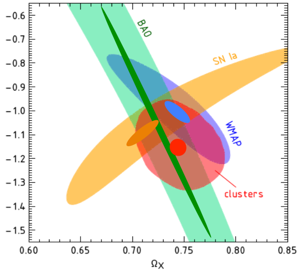

Reliability of cluster masses

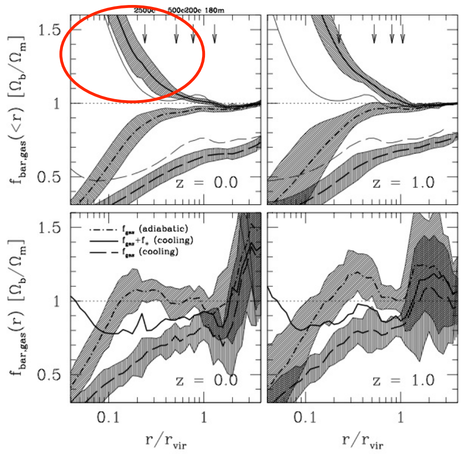

FIG. 3.—Differential (*bottom panels*) and cumulative (*top panels*) baryon and gas fraction profiles for the nine clusters used in our analysis at $z = 0$ (*left column*) and $z = 1$ (*right column*). The dot-dashed lines show the mean profiles in the adiabatic simulations averaged over eight clusters (CL2–CL9). The solid lines show the total mean baryon fraction (gas+stars) profile, while the long-dashed lines show the gas fraction profile in the simulations with cooling and star formation. The shaded bands show the 1 σ rms scatter around the mean for the eight clusters. The thin lines in the top panels show the corresponding profiles in the Coma-size cluster simulation (CL1). These profiles have not been used in the averages due to systematically different gas and baryon fractions. The vertical arrows in the top panels show the radii enclosing overdensities of 2500, 500, 200 (with respect to ρ_{crit}), and the overdensity of 180 with respect to the mean density.

- Kravtsov et al. simulations
  - DO include baryons, but …
  - DO NOT reproduce observed clusters, because they …
  - DO NOT include AGN feedback

Reliability of cluster masses

– critique of Vikhlinin et al., 2009 –

Cluster samples selected purely on X-ray flux / luminosity
– i.e. no morphological selection

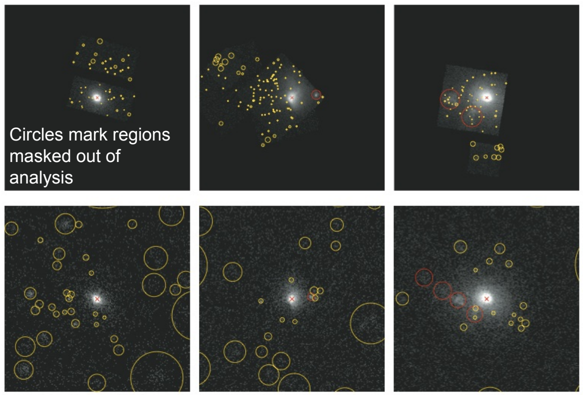

X-ray temperature and gas density measurement methods calibrated on over-cooled simulations

Mass-Y_X relation (predicted by over-cooled simulations to be reliable) used to convert X-ray observables to mass

Mass-Y_X relation measured for 17 “relaxed” clusters – meaning they look round

Figure 3. Typical examples of X-ray images for the low-redshift clusters (A85, A2163, and A2597 top to bottom). The left panels show the *Chandra* images (each panel is 50′ × 50′). *ROSAT* PSPC images (64′ × 64′) are shown on the right. Yellow circles show detected sources unrelated to the clusters; the general increase of their radius at large off-cluster distances reflects the degradation of the telescope PSF. The red circles indicate the cluster substructures that were removed from the profile analysis (Section 3.2). The red crosses mark the location of the adopted cluster centroid (Section 3.2).

Controlling cluster mass measurement systematics

Adopt a mass observable scaling relation of the form: $M = M_0 X^{\alpha}$

For simplicity assume there is no intrinsic scatter.

Error on normalization of relation will scale with sample size, N, and error on individual cluster mass measurements, $M_{cluster}$, like this:

$$\frac{\delta M_0}{M_0} \approx \frac{\delta M_{cluster}}{M_{cluster}} \frac{1}{\sqrt{N}}$$

Typical statistical errors on mass measurements are 20%

A sample of 50 – 100 clusters therefore yields a statistical error on normalisation of scaling relation of:

$$\frac{\delta M_0}{M_0} \approx 0.02 - 0.03$$

A useful benchmark goal is to control systematic errors to the same level – this has not yet been achieved / proven.

Lensing Constraints on Galaxy Cluster Mass and Structure

Graham P. Smith

gps@star.sr.bham.ac.uk

University of Birmingham

1. Primer on the physics of galaxy clusters
2. Galaxy clusters as cosmological probes
3. Galaxy clusters as gravitational lenses

Summary of Part 1

- Galaxy clusters contain:
  - a fair sample of the content of universe
  - DM, galaxies, intracluster stars, hot gas
- Galaxy clusters inhabit the exponential tail of the DM halo mass function
- Galaxy clusters are therefore powerful cosmological tools
- Cluster cosmology would be easy (and boring!) if clusters are self-similar
- Cluster masses can be inferred from X-ray (and optical) observations by assuming relationship between baryons and DM
- Departures from self-similarity → lots of interesting physics

Summary of Part 2

- Clusters are long-standing probes of cosmology
- Clusters can constrain dark energy in multiple ways:
  - growth of structure (number counts, mass function, clustering)
  - expansion history (f_{gas}, strong-lensing tomography)
- Main challenges:
  - control systematics in mass measurements
  - calibrate and understand departures from self-similarity
  - constrain evolution of cluster population
  - understand selection biases
- Gravitational lensing is a promising tool …

Part 3

Galaxy Clusters as Gravitational Lenses

Overview

- Strong lensing by clusters
  - Simple mass measurements
  - Parametric mass measurements
  - Substructure of cluster cores
  - Example results (emphasising samples)
- Weak lensing by clusters
  - From raw data to cosmology
  - X-ray/lensing mass comparison
  - M_{WL}-observable scaling relations

Lensing by Galaxy Clusters

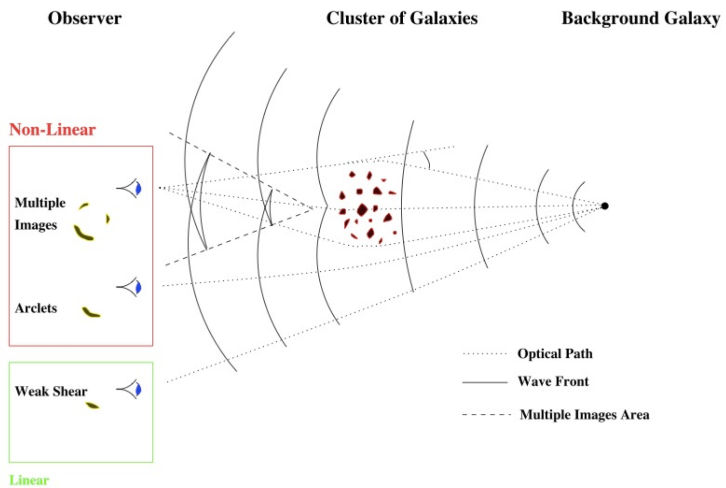

Credit: Jean-Paul Kneib

Cluster Strong Lensing

Einstein radius depends on lensing efficiency and mass distribution

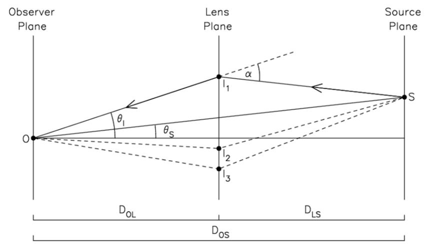

$$\theta_{\rm I} = \theta_{\rm S} + \frac{D_{\rm LS}}{D_{\rm OS}}\alpha(\theta_{\rm I})$$

For a singular isothermal sphere of velocity dispersion σ:

$$\theta_E = \frac{4\pi\sigma^2}{c^2}\frac{D_{LS}}{D_{OS}} \approx \left(\frac{\sigma}{1000\ \text{km/s}}\right)^2 \left(\frac{D_{LS}/D_{OS}}{0.4}\right) 20\text{arcsec}$$

$$R_E = D_{OL}\theta_E = \frac{4\pi\sigma^2}{c^2}\frac{D_{OL}D_{LS}}{D_{OS}} = \frac{4\pi\sigma^2 D}{c^2} \approx \left(\frac{\sigma}{1000\ \text{km/s}}\right)^2 \left(\frac{D}{500\text{Mpc}}\right) 70\text{kpc}$$

Simplest mass measurement

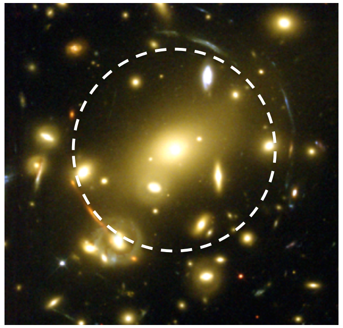

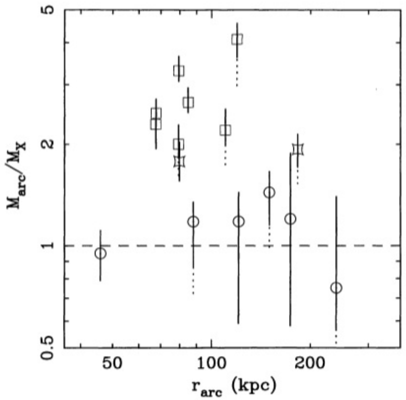

Allen 1998; Miralda-Escude & Babul, 1995

$$M(<R_E) = \Sigma_{crit}\, \pi R_E^2$$

$$\Sigma_{crit} = \frac{c^2}{4\pi G}\, \frac{D_{OS}}{D_{OL} D_{LS}}$$

Questions

- How reliable is the assumption of circular symmetry?
- Strongly distorted single image or bona fide multiple-imaging?
- How sensitive is the measurement to the source redshift?
- How to combine several multiple image systems?

Circular Symmetry?

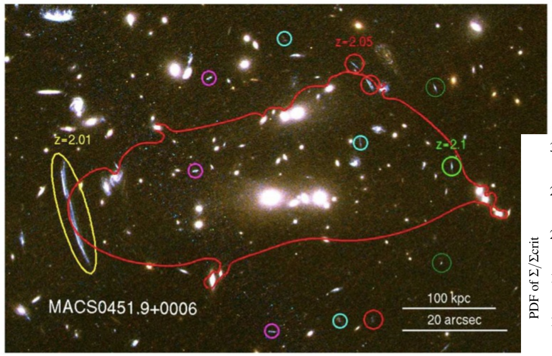

From Kneib & Natarajan 2011; courtesy of Johan Richard

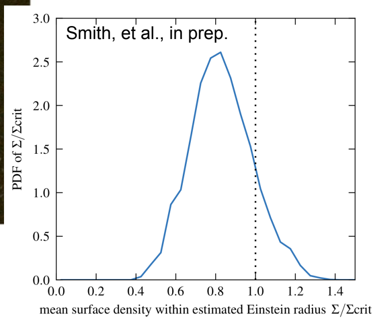

Single or multiple images?

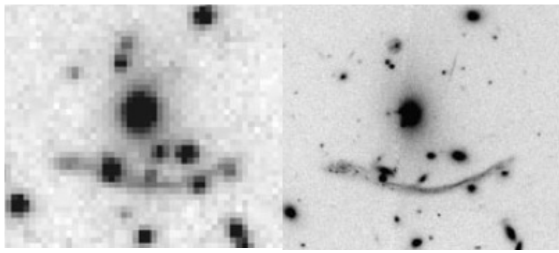

If the arc is not multiply-imaged, then the mass estimate is an upper limit:

$$\Sigma(<R_{arc}) < \Sigma_{crit}$$

$$M(<R_{arc}) < \pi R_{arc}^2\, \Sigma_{crit}$$

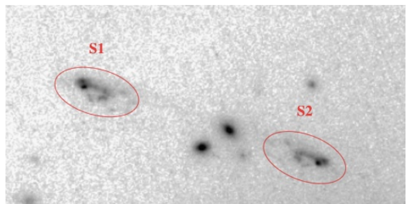

Adapted from: Kneib & Natarajan, 2011

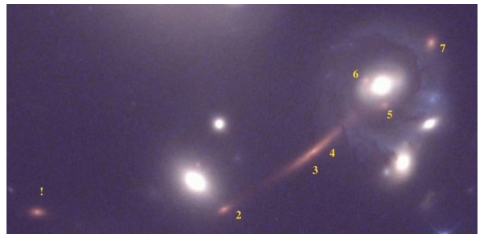

Sensitivity to redshift?

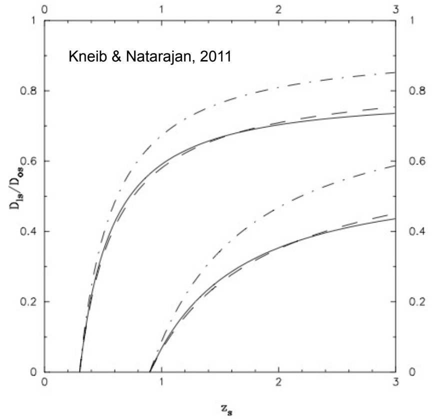

Fig. 5 Lensing efficiency $\mathcal{E} = D_{LS}/D_{OS}$ for a given lens as a function of source redshift z_S for different cosmologies. The two sets of curves correspond to two different lens redshifts $z_L = 0.3$ and $z_L = 0.9$ and the *solid lines* correspond to $\Omega_m = 0.1$, $\Omega_\Lambda = 0$; the *dashed line* to $\Omega_m = 1$, $\Omega_\Lambda = 0$; and the *dashed-dotted line* to $\Omega_m = 0.1$, $\Omega_\Lambda = 0.9$

Calibrating the accuracy of M(<R$_E$)

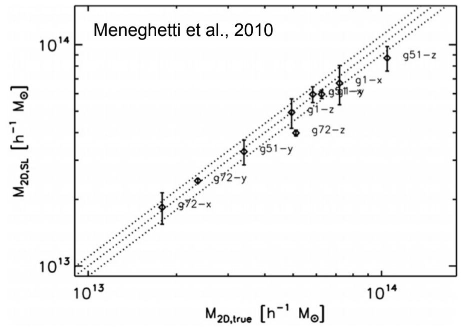

Fig. 13. The projected masses estimated through the strong lensing analysis vs. the corresponding true masses of the lenses. The dotted lines correspond to $M_{2D,SL} = M_{true}$ and to $M_{2D,SL} = M_{true} \pm 10\%$. The masses are measured within a circle centered on the BCG and having a radius equal to the mean distance of the lensing constraints from the cluster center.

Large Einstein Radii: A Problem for LCDM(?)

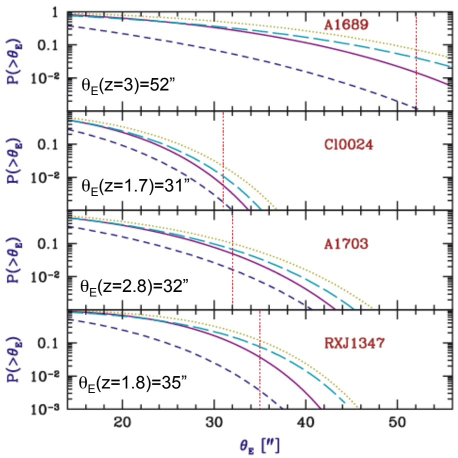

- Most spectacular SL clusters are ~2σ outliers when compared with simulations
- Interpretation?
  - Early collapse of cluster cores
  - Modify properties of dark matter?
  - Modify slope of primordial power spectrum?
  - Primordial non-Gaussianity?
- Better to compare the **"full"** distribution of observed and simulated SL clusters

Broadhurst & Barkana (2008)

Einstein radius distribution

Richard, GPS, et al., 2010, MNRAS, 404, 325

- Log-normal θ_E distribution for strong-lensing/X-ray selected clusters
- Observed and theoretical distributions offset by ~1σ
- Future needs:
  - Larger observed sample
  - Better calibration of selection functions
  - Full SL+WL models to improve comparison with simulations
  - More realistic simulations (BCG formation)

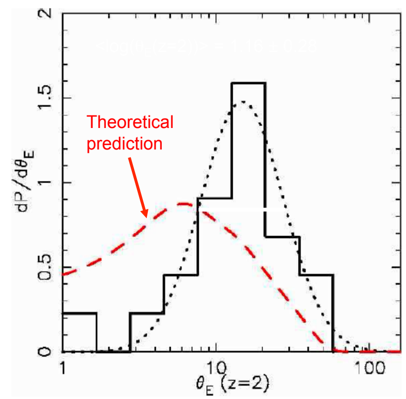

Fitting models to SL constraints

- Choose a projected mass distribution
- Calculate deflection field
- Calculate predicted positions of images
- Compare predicted and observed positions
- Change mass distribution
- Decide to stop
- Repeat with different model?
- Choose model (i.e. how complex?)

David and Leon's lectures

MCMC
Bayesian evidence
Tom's lecture

Jullo et al., 2007
Smith et al., 2009
Limousin et al., 2012

LENSTOOL: http://www.oamp.fr/cosmology/lenstool/

Parameterising the mass distribution

- One singular isothermal sphere/ellipse
  - Over-produces central images
  - X-ray surface brightness profiles are curved
- One non-singular sphere/ellipse
  - Images reproduced to ~1 – 5 arcsec precision
  - Corresponds to deflection angle of galaxies/groups
- Multiple non-singular cluster/group/galaxy-scale masses
  - Images reproduced to ~0.1 – 0.5 arcsec precision
  - Precision depends on number of constraints

$$\phi_{\rm total} = \sum_{\rm i} \phi^{\rm i}_{\rm extended} + \sum_{\rm j} \phi^{\rm j}_{\rm galaxies}$$

Parameterising the mass distribution

"weak" shear + bright galaxies | multiple-images | X-ray flux | mass map

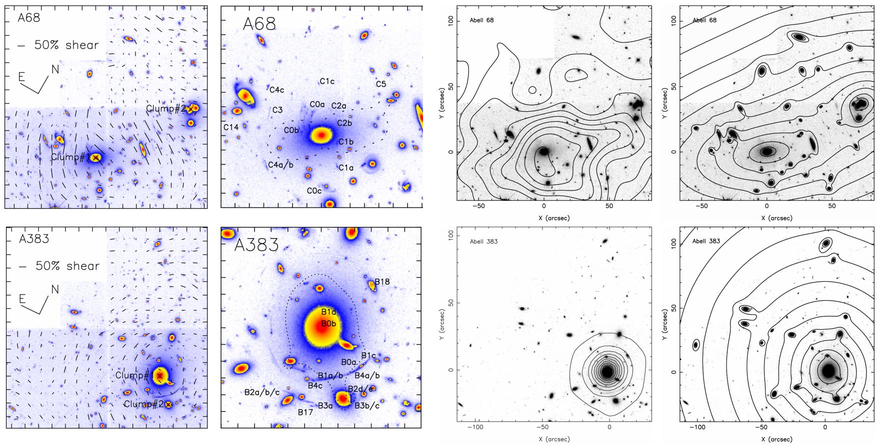

Examples from GPS, Kneib, et al. 2005 (5 SL clusters in total)

Parameterising the mass distribution

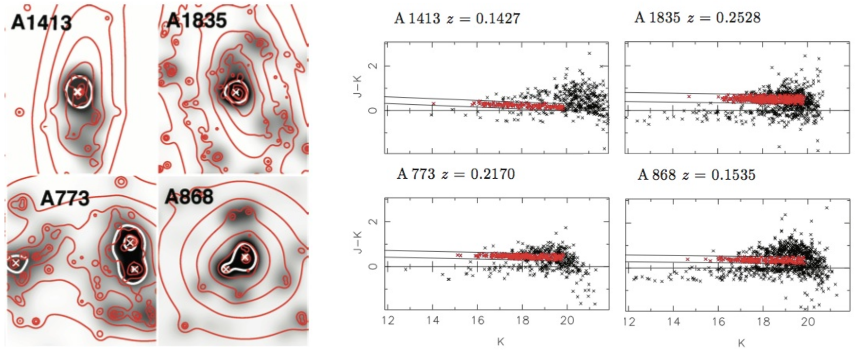

Examples from Richard, GPS, Kneib, et al., 2010 (20 SL clusters from LoCuSS)

See also: Paraficz et al., 2012 – explicit inclusion of ICM in a SL model

Parameterising the mass distribution

- Extended halos:
  - Navarro, Frenk, White (1997) profile
    Bartelmann (1996), Golse & Kneib (2002), Sand et al., (2008)
  - Smoothly truncated pseudo-isothermal elliptical mass distribution (PIEMD)
    Kassiola & Kovner (1993), Kneib et al., (1996), Jean-Paul's lectures

$$\Sigma(x, y) = \frac{\sigma_0^2}{2G}\frac{r_{\rm cut}}{r_{\rm cut} - r_{\rm core}}\left[\frac{1}{(r_{\rm core}^2 + \rho^2)^{1/2}} - \frac{1}{(r_{\rm cut}^2 + \rho^2)^{1/2}}\right]$$

$$\rho^2 = [(2-e)\,(x - x_c)/2]^2 + [(2-e)\,(y - y_c)/(2-2e)]^2$$

- Choice depends on what question you ask:
  - Questions about total mass distribution – NFW and PIEMD agree within errors (Richard, GPS, Kneib, et al., 2010)
  - Questions about the distribution of DM – must use NFW (e.g. Sand et al., 2008)
- Typical PIEMD parameter values:

$$300 < \sigma_0 < 1300 \text{ km/s}, \quad 20 < r_{core} < 150 \text{ kpc}, \quad r_{cut} = 1 \text{ Mpc}$$

NFW or PIEMD?

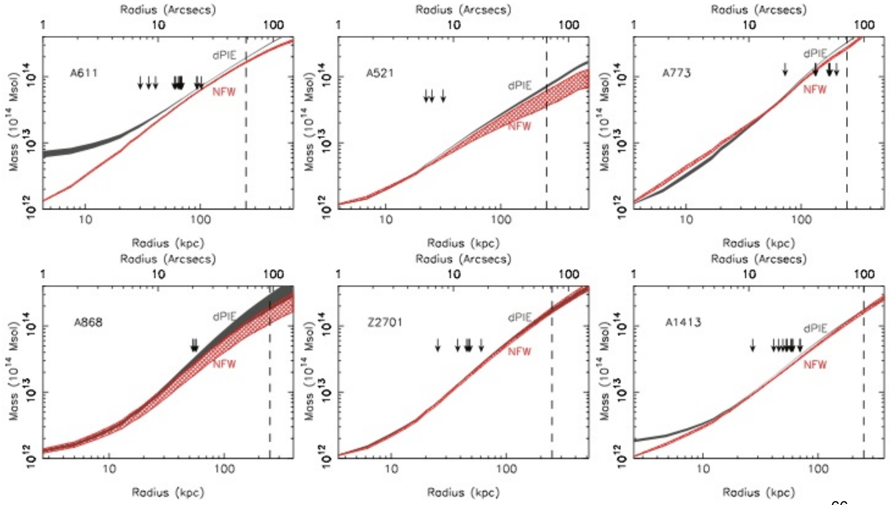

Examples from Richard, GPS, Kneib, et al., 2010 (20 SL clusters from LoCuSS)

Parameterising the mass distribution

- Parameterise galaxy-scale halos as PIEMDs
- Individually optimise parameters (generally just velocity dispersion) of galaxies close to multiple-images
- Scale mass of other galaxies (can be 10s of galaxies) on their luminosity

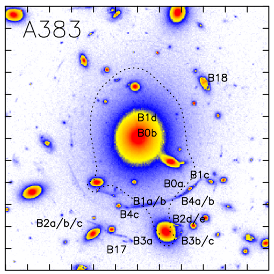

$$\sigma_0 = \sigma_0^\star \left(\frac{L}{L^\star}\right)^{1/4},$$

$$r_{\rm core} = r_{\rm core}^\star \left(\frac{L}{L^\star}\right)^{1/2},$$

$$r_{\rm cut} = r_{\rm cut}^\star \left(\frac{L}{L^\star}\right)^{\alpha}.$$

Fitting models to SL constraints

- Choose a projected mass distribution
- Calculate deflection field
- Calculate predicted positions of images
- Compare predicted and observed positions
- Change mass distribution
- Decide to stop
- Repeat with different model?
- Choose model (i.e. how complex?)

David and Leon's lectures

MCMC
Bayesian evidence
Tom's lecture

Jullo et al., 2007
Smith et al., 2009
Limousin et al., 2012

MACSJ1149.5+2233

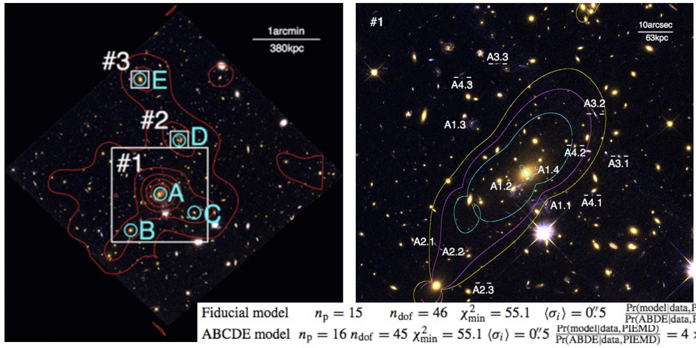

Fiducial model	$n_p = 15$	$n_{dof} = 46$	$\chi^2_{min} = 55.1$	$\langle\sigma_i\rangle = 0.''5$	$\frac{Pr(model\|data, PIEMD)}{Pr(ABDE\|data, PIEMD)} = 1$
ABCDE model	$n_p = 16$	$n_{dof} = 45$	$\chi^2_{min} = 55.1$	$\langle\sigma_i\rangle = 0.''5$	$\frac{Pr(model\|data, PIEMD)}{Pr(ABDE\|data, PIEMD)} = 4 \times 10^{-2}$
ABD model	$n_p = 13$	$n_{dof} = 48$	$\chi^2_{min} = 471.3$	$\langle\sigma_i\rangle = 1.''4$	$\frac{Pr(model\|data, PIEMD)}{Pr(ABDE\|data, PIEMD)} = 2 \times 10^{-96}$
ABE model	$n_p = 14$	$n_{dof} = 47$	$\chi^2_{min} = 86.8$	$\langle\sigma_i\rangle = 0.''6$	$\frac{Pr(model\|data, PIEMD)}{Pr(ABDE\|data, PIEMD)} = 4 \times 10^{-12}$
ADE model	$n_p = 14$	$n_{dof} = 47$	$\chi^2_{min} = 110.9$	$\langle\sigma_i\rangle = 0.''8$	$\frac{Pr(model\|data, PIEMD)}{Pr(ABDE\|data, PIEMD)} = 8 \times 10^{-13}$
AB model	$n_p = 12$	$n_{dof} = 49$	$\chi^2_{min} = 493.8$	$\langle\sigma_i\rangle = 1.''5$	$\frac{Pr(model\|data, PIEMD)}{Pr(ABDE\|data, PIEMD)} = 6 \times 10^{-93}$
AD model	$n_p = 12$	$n_{dof} = 49$	$\chi^2_{min} = 539.5$	$\langle\sigma_i\rangle = 1.''7$	$\frac{Pr(model\|data, PIEMD)}{Pr(ABDE\|data, PIEMD)} = 2 \times 10^{-102}$
AE model	$n_p = 13$	$n_{dof} = 48$	$\chi^2_{min} = 130.7$	$\langle\sigma_i\rangle = 0.''9$	$\frac{Pr(model\|data, PIEMD)}{Pr(ABDE\|data, PIEMD)} = 4 \times 10^{-20}$
A model	$n_p = 11$	$n_{dof} = 50$	$\chi^2_{min} = 551.1$	$\langle\sigma_i\rangle = 1.''8$	$\frac{Pr(model\|data, PIEMD)}{Pr(ABDE\|data, PIEMD)} = 5 \times 10^{-107}$

GPS, Ebeling, Limousin, Kneib, et al., 2009

Non-analytic modeling schemes

- Basic idea:
  - Parameterise the mass distribution as a grid of pixels
  - Pixel values are the model parameters – i.e. “non-parametric” is misnomer
- Advantages:
  - Greater flexibility helps to explore complicated merging clusters
- Disadvantages:
  - Arbitrarily good fits can be achieved – how robust?
  - Known (visible) mass not included explicitly
  - Strong lensing signal is typically sparse – not true for a few spectacular systems
  - Additional assumptions invoked: e.g. smoothest mass distribution, mass positivity
- Examples:
  - Bradac et al., 2005; Diego et al. 2005, 2007; Saha and Williams 1997; Coe et al. 2010; …
- Hybrid analytic+non-analytic schemes also under development:
  - Jullo & Kneib, 2009; Paraficz et al., 2012

Substructure in cluster cores

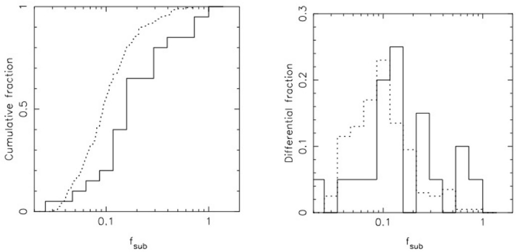

Richard, GPS, et al., 2010

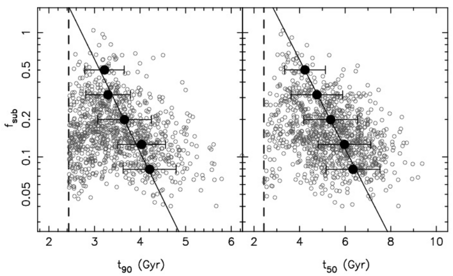

GPS & Taylor, 2008

X-ray/lensing mass comparison

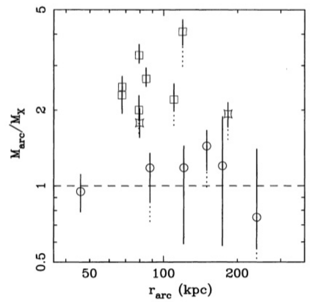

Allen 1998; Miralda-Escude & Babul, 1995

$$\left\langle \frac{M_{SL}}{M_X} \right\rangle = 1.3 \pm 0.1$$

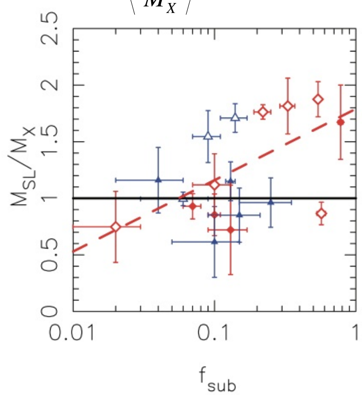

Richard, GPS, et al., 2010

Recommended further reading

- Constraining the slope of cluster density profiles
  - with radial arcs: Fort et al., Smith et al., 2001;
  - with radial arcs + stellar dynamics: Gavazzi et al., ; Sand et al., 2004, 2008;
  - with radial arcs + dynamics + … : Newman et al.,
  - with rare image configurations: Limousin et al.
- Joint fitting of SL + X-ray + SZ data:
  - Morandi et al., …
  - Mahdavi et al., …
- *Will be completed before notes go online!*

Lensing by Galaxy Clusters

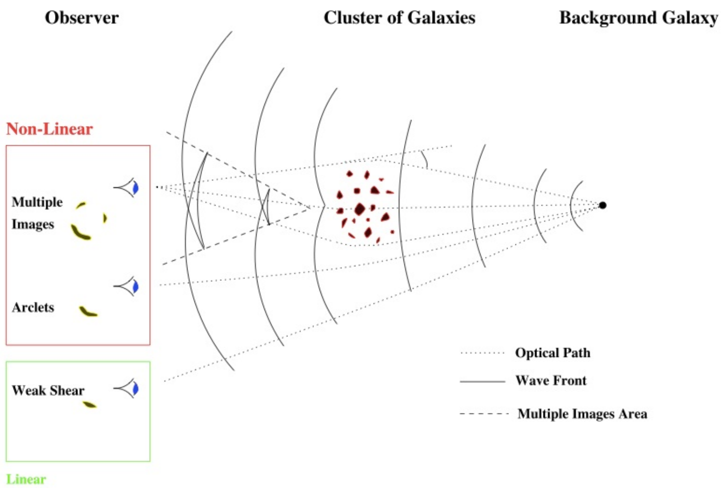

Credit: Jean-Paul Kneib

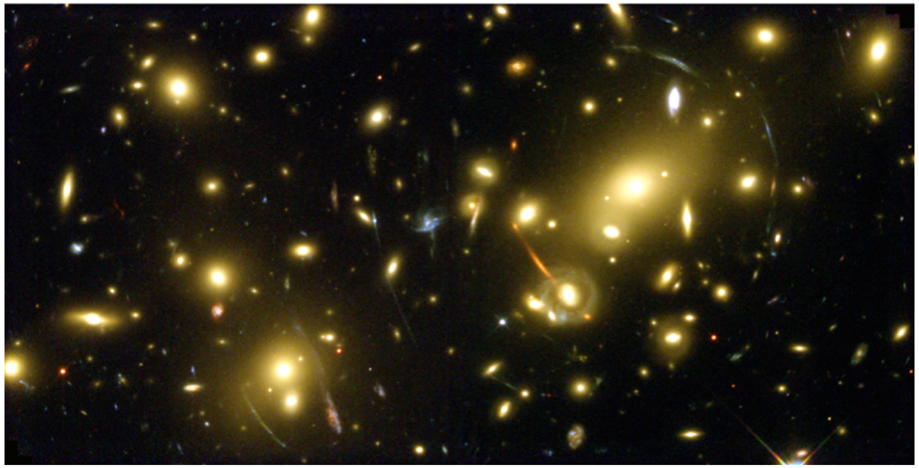

Strong- and weak-lensing

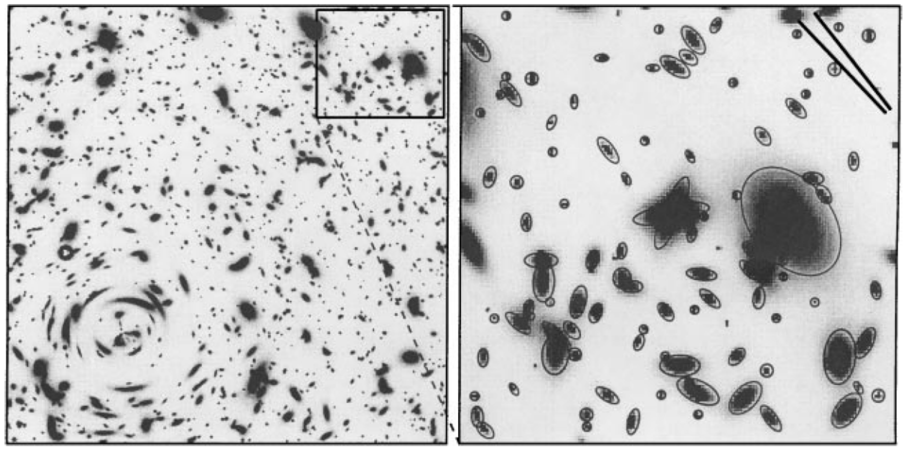

Mellier, 1999, ARA&A, 37, 127

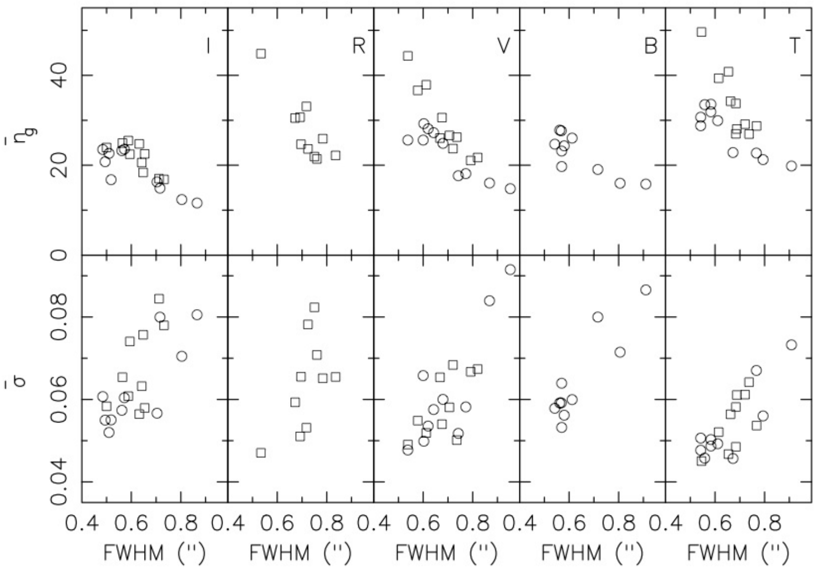

Fig. A.1. Plotted above are the number density of background galaxies usable for shear measurements (*top panels*) and the rms shear noise-level per sq. arcminute per shear component from these galaxies (*bottom panels*) as a function of PSF size for the four observed passbands (I, R, V, and B) and the combined catalog (T). The 2-h exposure time images of the high-z clusters are plotted as squares, while the 45-min exposure time images of the lower redshift clusters are plotted as circles.

Clowe et al., 2006 (EDISCS)

Example weak-lensing data

Okabe, Takada, Umetsu, Futamase, GPS, 2010, PASJ, 62, 811

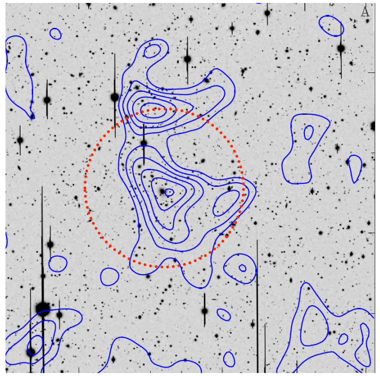

See David's lecture: map-making

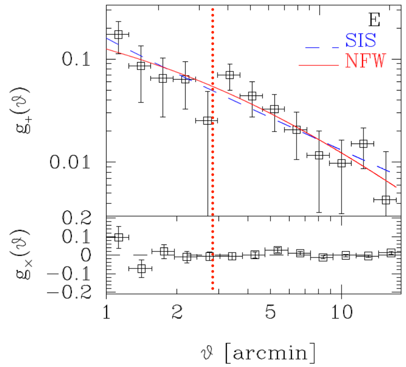

See David/Tom's lectures: reduced shear, E/B-modes (45 degree test)

Extracting mass from WL data

- Fit an analytic density profile
  - e.g. SIS, CPL, NFW, …
- Aperture mass densitometry
  - Fahlman et al., 1994; Clowe et al., 1998; Hoekstra 2007; Okabe et al., 2010
- Projected density contrast, $\Delta\Sigma$
  - Mandelbaum et al., 2005, 2010; Johnston et al., 2007; Leauthaud et al., 2010; High et al., 2012

Are density profiles curved?

Okabe, Takada, Umetsu, Futamase, GPS, 2010, PASJ, 62, 811

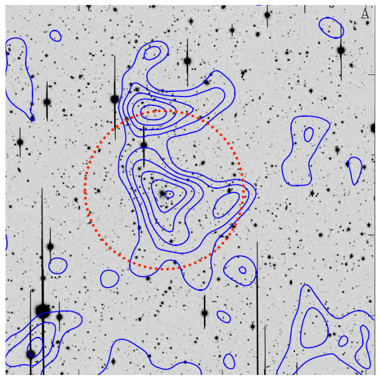

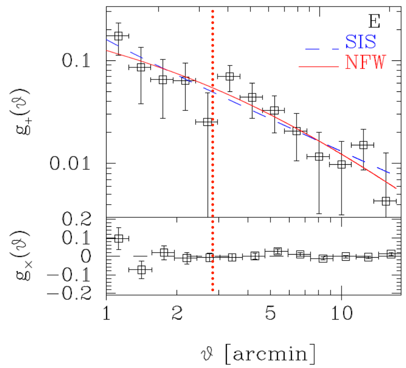

Stacked weak-lensing

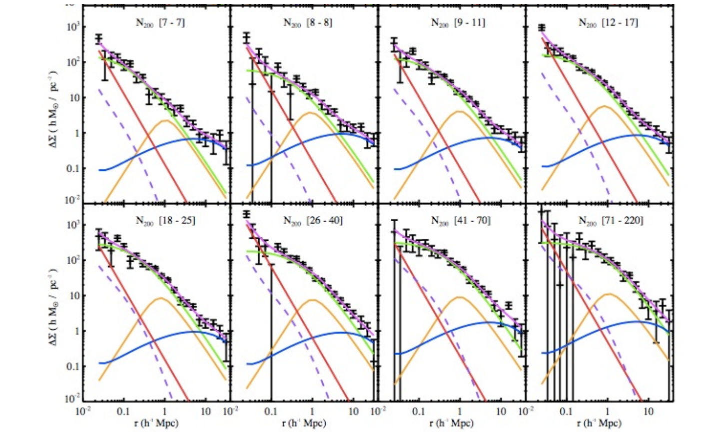

FIG. 8.— Model fits to $\Delta\Sigma(R)$ for the 12 N_{200} richness bins The model components are the NFW halo profile (green), miscentered halo component (orange), the central BCG (red), neighboring halos (blue); the non-linear contribution (purple dashed). The magenta curves show the sum of these components for the best-fit models in each bin.

Johnston et al., 2007

Are cluster density profiles curved?

Okabe, Takada, Umetsu, Futamase, GPS, 2010, PASJ, 62, 811

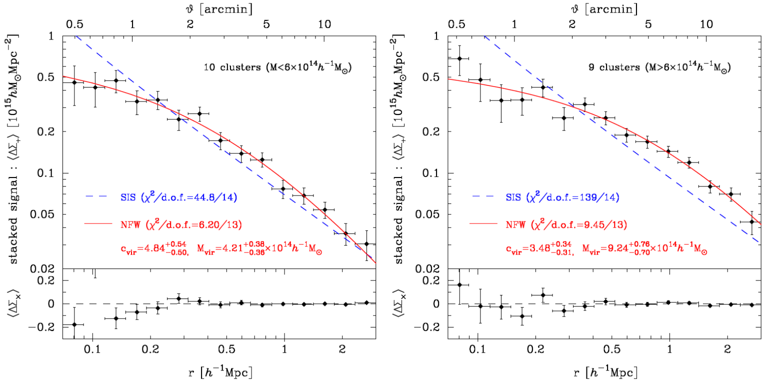

- SIS profile rejected:
  - 6σ (M_{vir}<6E14$M_\odot$/h)
  - 11σ (M_{vir}>6E14$M_\odot$/h)

Are clusters over-concentrated?

Okabe, Takada, Umetsu, Futamase, GPS, 2010, PASJ, 62, 811

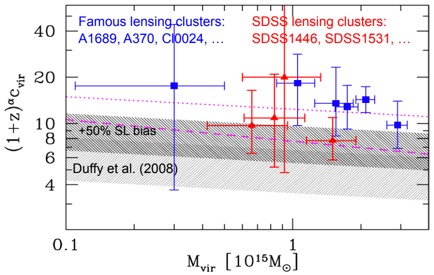

Oguri et al., (2009)

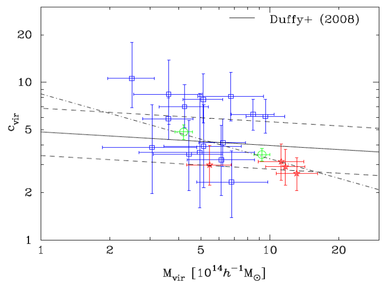

- $10^{15}M_\odot$/h clusters:
  - <c_{vir}> = 3.48+1.65-1.15
  - Inconsistent with c~10 at ~4σ

From raw data to cosmology

- Raw data → galaxy shapes
  - See David and Tom's lectures
- Galaxy shapes → shear signal
  - Redshift distribution of faint galaxies
- Shear signal → M_{WL}
  - Model choice
- M_{WL} → cosmological constraints
  - M_{WL} is itself a "mass proxy"

Basic idea: faint cluster galaxies (and foreground galaxies) can dilute the measured shear signal

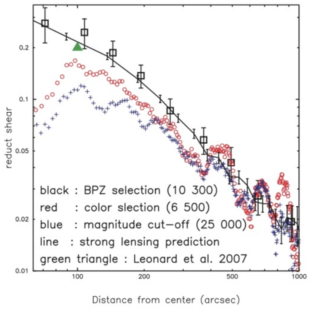

Limousin et al., 2007 – A1689

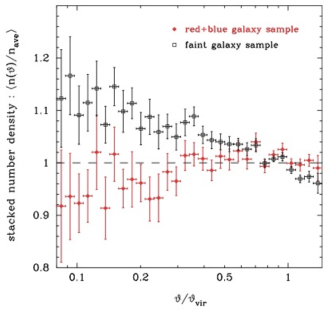

Okabe et al., 2010 – 30 clusters

Galaxy shapes → shear signal

Redshift distribution of faint galaxies

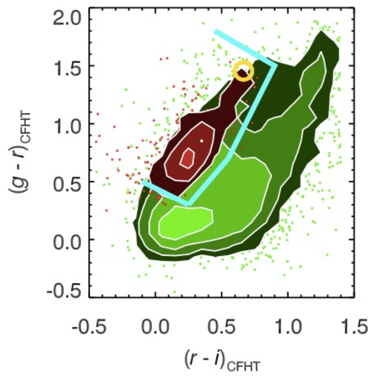

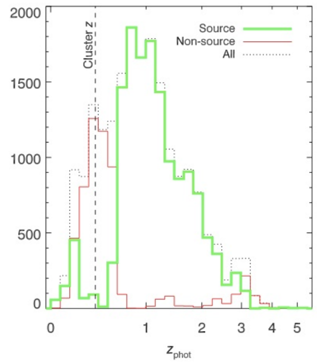

High et al., 2012 – 5 clusters from SPT

See also “weighing the giants”: arXiv:1208.0597, 1208.0602, 1208.0605

Shear signal → M_{WL}

Model Choice

Basic idea: triaxiality and substructure cause systematic errors in WL mass measurement of individual clusters

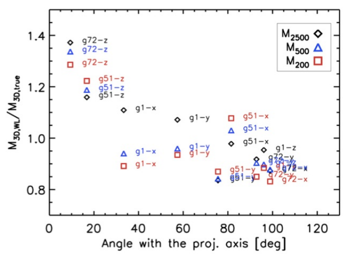

Fig. 17. Ratio between estimated and true lensing masses as a function of the angle between the major axis of the cluster inertia ellipsoid and the axis along which the mass distribution is projected. The results are shown for the lensing masses obtained with the SL+WL method. Squares, triangles and diamonds indicate the mass measurements at R_{200}, R_{500}, and R_{2500}, respectively.

Meneghetti et al., 2010

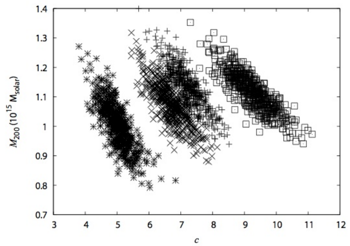

Figure 2. The concentration parameter c and mass M_{200} for best-fitting single NFW haloes to (i) single fiducial halo (∗), (ii) 10 per cent of mass in secondary halo, $c_s = 7$ (x), (iii) same as (ii) but with 20 per cent in secondary halo (+), and (iv) 10 per cent of mass in each of two $c_s = 10$ haloes (□). Each point within a group corresponds to a different noise realization of random unlensed galaxy positions and ellipticities.

King & Corless 2007

See also: Becker & Kravtsov 2011 ; Bahe et al., 2012; Corless & King 2007, 2008, 2009

M_{WL} → cosmological constraints

M_{WL} is itself a mass proxy

- Accurately calibrated M_{WL}-observable scaling relation is not enough …
- M_{WL}-M_{true} relation is also required – see previous slide
- Open questions:
  - How to define mass? 3D, 2D, over-density, fixed radius, …
  - How do alternatives perform relative to realistic hydro simulations? (they are coming!)

Aside on M_X systematics

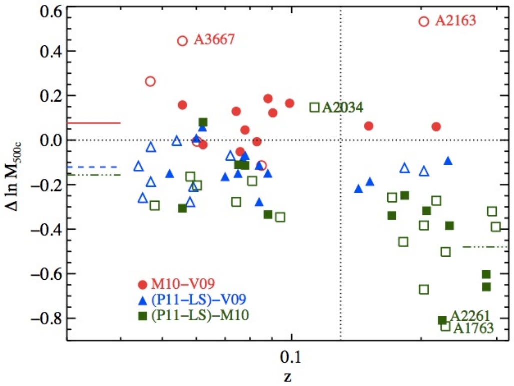

FIG. 1.— Differences in M_{500} between clusters shared by the Vikhlinin et al. (2009a, V09), Mantz et al. (2010b, M10), and Planck Collaboration (2011b, P11-LS) samples. Filled circles are relaxed/cool-core clusters, while open circles are non-relaxed or non cool-core systems. The small horizontal lines along the y axis mark the average mass offset for each of the three cross-comparisons: M10–V09 (solid red), (P11-LS)–V09 (dashed blue), (P11-LS)–M10 (dot-dashed green). For the (P11-LS)–M10 comparison, we show averages computed separately for low and high redshift systems, split at $z = 0.13$ (vertical dotted line). The low and high redshift averages are displaced on the left and right axes respectively. All averages are computed using only relaxed/cool-core systems. Clusters labeled are discussed in § 3.1.2

Rozo et al., 2012

M_X/M_{WL} comparison

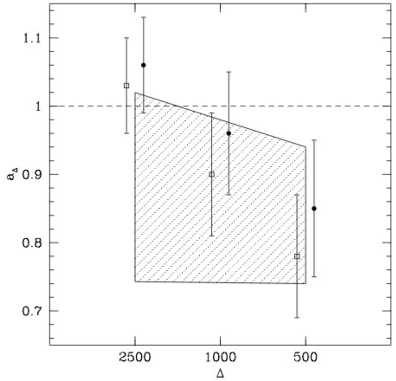

CCCP: Mahdavi et al., 2008

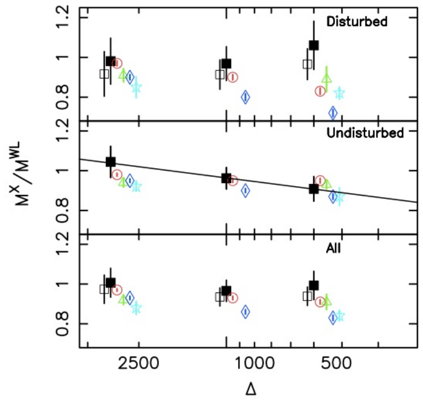

LoCuSS: Zhang et al., 2010

M_{WL}/X-ray scaling relations

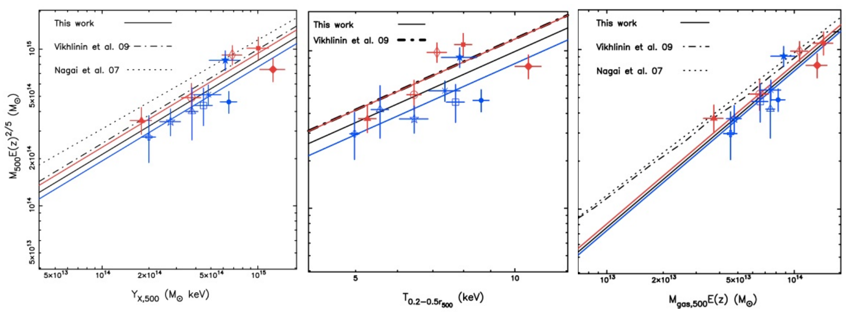

Okabe et al. (2010) – Lowest scatter X-ray observable appears to be M_{gas} (but the sample is small – so far!) – **NOT Y_X**

See also: Mahdavi et al. submitted

M_{WL}/SZ scaling relations

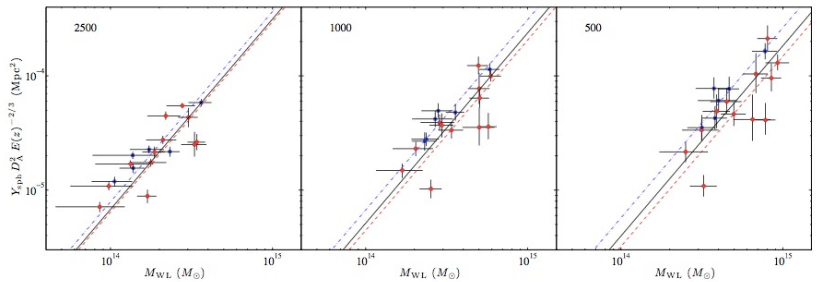

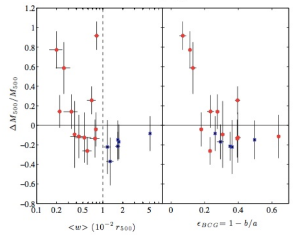

Marrone, GPS, et al., 2012:
- 20% scatter on MWL-Y relation
- BCG ellipicity indicates DM halo orientation?

See also: Hoekstra et al., 2012

Summary

- “Creative tension” between lensing and X-ray approaches is very stimulating
- Both communities making good progress on controlling systematic errors
- Lots of opportunities/work remains to be done
- Lots of data arriving in the next decade and more
- Prospects are strong for cluster cosmology (and learning lots of interesting astrophysics!)